

# Investigation of Reaction Conditions for Optimal Germanium Nanoparticle Production by a Simple Reduction Route

Hsiang Wei Chiu and Susan M. Kauzlarich\*

Department of Chemistry, One Shields Avenue, University of California Davis, Davis California 95616

Received September 20, 2005. Revised Manuscript Received November 23, 2005

Various reaction conditions, such as reductant, time, procedure, concentration, and temperature, were investigated with the aim of finding a simple, optimized synthetic route for the synthesis of crystalline germanium nanoparticles. Results from these studies indicate that sodium naphthalide is an ideal reductant and that the reaction is virtually complete within 10 min. Furthermore, it was observed that a two-pot synthesis resulted in a cleaner, narrower distribution of nanoparticle size and that the narrowest size distribution ( $\sim 20\%$ ) was produced when a dilute Na(naphth) in glyme mixture was utilized. The optimum initial reduction temperature was found to be  $0^\circ\text{C}$ . It was also shown that concentration and temperature play an important role in controlling nanoparticle size. The best reaction conditions, as stated above, produced nanoparticles with a size dispersion of  $\sim 20\%$  when combined. Transmission electron microscopy (TEM), selected-area electron diffraction (SAED), high-resolution TEM (HRTEM), energy-dispersive X-ray spectroscopy (EDS), X-ray powder diffraction (XRD), and chemical analysis were used to characterize the nanoparticles.

## Introduction

The synthesis of high-quality semiconductor quantum dots (QDs) is important because of possible applications in nanotechnology and biology.<sup>1,2</sup> Much progress has been made in the chemical syntheses of groups II–VI and III–V colloidal QDs,<sup>3,4</sup> as well as of single-phase and gram-scale Au nanoparticles (NPs);<sup>5</sup> however, less progress has been made in Ge NP synthesis, which is still in the developmental stage. At present, there are two major directions for the synthesis of Ge NPs: high-temperature, high-pressure and low-temperature, ambient-pressure. Both approaches arise from the unique feature that group IV Ge structures can exist as either amorphous or crystalline materials. Typically, it is found that low-temperature synthetic routes favor the kinetic product; therefore, high-temperature routes are often employed to obtain the thermodynamically favored product. Results from this group,<sup>6–9</sup> along with others,<sup>10–14</sup> show that

crystalline Ge NPs can be obtained not only from the high-temperature, high-pressure solution routes, but also from low-temperature, ambient-condition routes.<sup>10–13,15</sup>

This group has previously demonstrated that crystalline Ge NPs can be prepared via reduction routes.<sup>15</sup> We have shown that room-temperature, butyl-capped Ge NPs are crystalline by electron microscopy studies and that, when surface termination is removed under a high-temperature vacuum, the NPs become amorphous.<sup>15</sup> We also demonstrated that these amorphous nanoparticles crystallize at  $561^\circ\text{C}$  and subsequently melt at  $925^\circ\text{C}$ .<sup>15</sup>

Classical studies by La Mer and Dinegar<sup>16</sup> assume that the production of nanoparticles results from a short nucleation burst followed by diffusional growth of the nuclei to form identical, finely dispersed particles. With the increasing availability of monodisperse colloids of different shapes, it is evident that the nucleation-burst/diffusional-growth mechanism alone cannot explain many observed experimental findings. Thus, the formation of monodisperse colloids poses two major challenges: first, the difficulty of maintaining particle morphology and shape formed by the interplay of the nucleation and aggregation processes and, second, the difficulty of optimizing size-selection mechanisms.<sup>17,18</sup> Morphology-, shape-, and size-selection mechanisms have been

\* Corresponding author. E-mail: smkauzlarich@ucdavis.edu.

- (1) Alivisatos, A. P. *Science* **1996**, *271*, 933–937.
- (2) Murray, C. B.; Kagan, C. R.; Bawendi, M. G. *Annu. Rev. Mater. Sci.* **2000**, *30*, 545–610.
- (3) Murray, C. B.; Norris, D. J.; Bawendi, M. G. *J. Am. Chem. Soc.* **1993**, *115*, 8706–8715.
- (4) Peng, X.; Wickham, J.; Alivisatos, A. P. *J. Am. Chem. Soc.* **1998**, *120*, 5343–5344.
- (5) Jana, N. R.; Peng, X. *J. Am. Chem. Soc.* **2003**, *125*, 14281.
- (6) Tanke, R. S.; Kauzlarich, S. M.; Patten, T. E.; Pettigrew, K. A.; Murphy, D. L.; Thompson, M. E.; Lee, H. W. H. *Chem. Mater.* **2003**, *15*, 1682–1689.
- (7) Taylor, B. R.; Fox, G. A.; Hope-Weeks, L. J.; Maxwell, R. S.; Kauzlarich, S. M.; Lee, H. W. H. *Mater. Sci. Eng.* **2002**, *B96*, 90–93.
- (8) Taylor, B. R.; Kauzlarich, S. M.; Delgado, G. R.; Lee, H. W. H. *Chem. Mater.* **1999**, *11*, 2493–2500.
- (9) Taylor, B. R.; Kauzlarich, S. M.; Lee, H. W. H.; Delgado, G. R. *Chem. Mater.* **1998**, *10*, 22–24.
- (10) Fok, E.; Shih, M.; Meldrum, A.; Veinot, J. G. C. *Chem. Commun.* **2004**, 386–387.
- (11) Hope-Weeks, L. J. *Chem. Commun.* **2003**, 2980–2981.

- (12) Wang, W.; Huang, J.; Ren, Z. *Langmuir* **2005**, *21*, 751–754.
- (13) Wilcoxon, J. P.; Provencio, P. P.; Samara, G. A. *Phys. Rev. B: Condens. Matter Mater. Phys.* **2001**, *64*, 035417–035419.
- (14) Lu, X.; Korgel, B. A.; Johnston, K. P. *Nanotechnology* **2005**, *16*, 389–394.
- (15) Chiu, H. W.; Chervin, C. N.; Kauzlarich, S. M. *Chem. Mater.* **2005**, *17*, 4858–4864.
- (16) La Mer, V. K.; Dinegar, R. H. *J. Am. Chem. Soc.* **1950**, *72*, 4847–4854.
- (17) Trindade, T.; O'Brien, P.; Pickett, N. L. *Chem. Mater.* **2001**, *13*, 3843–3858.
- (18) Privman, V.; Goia, D. V.; Park, J.; Matijević, E. *J. Colloid Interface Sci.* **1999**, *213*, 36–45.

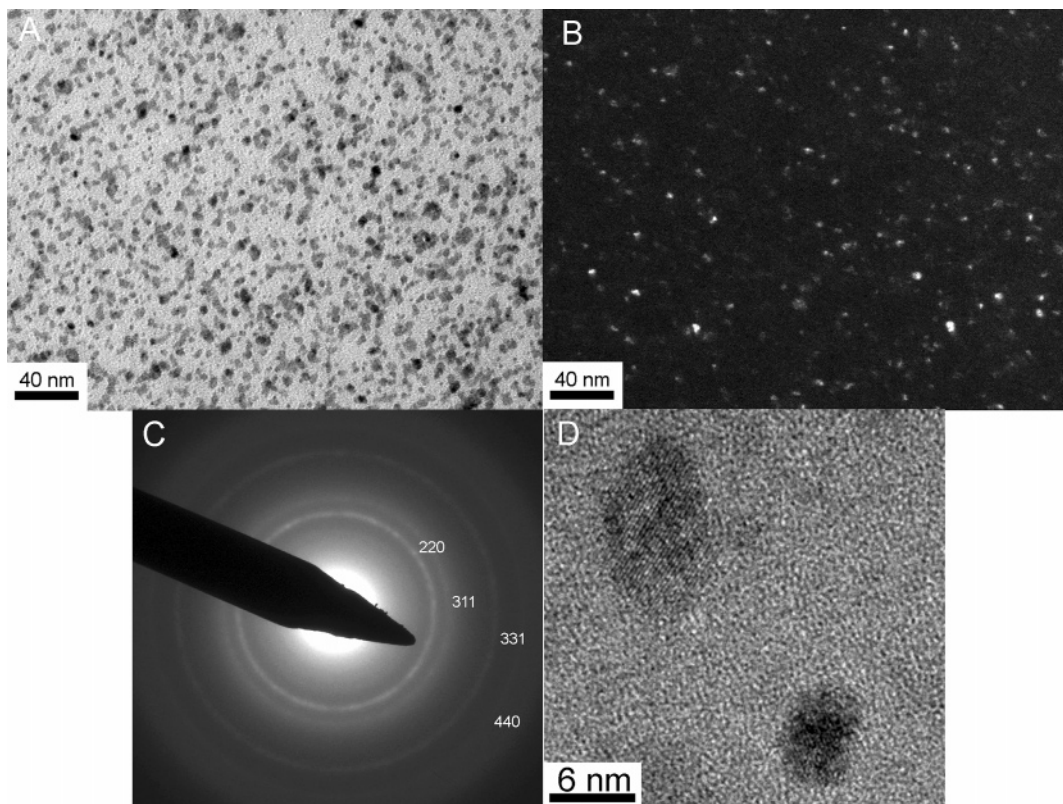


**Figure 1.** (A) Bright-field and (B) dark-field TEM micrographs, (C) selected-area electron diffraction (SAED) pattern, and (D) high-resolution TEM micrograph of butyl-terminated as-prepared Ge NPs.

intensively studied and are well understood for the synthesis of groups II–VI semiconductors, such as CdS,<sup>3,4,19</sup> and ZnS,<sup>20,21</sup> silver,<sup>22,23</sup> and TiO<sub>2</sub> particles.<sup>24,25</sup> However, to date, detailed studies on the formation of group IV NPs by any colloidal methods are minimal.

In this article, we attempt to fill some of the void by investigating the effects of various reaction conditions on *n*-butyl-terminated Ge NPs. Our aim is to develop a simple, optimized synthetic method for the production of Ge NPs that not only allows for size and shape control, but also permits the maintenance of high crystallinity and monodispersity within the materials.

### Experimental Section

**Materials.** Ethylene glycol dimethyl ether (glyme) (Acros, >99%) was dried and distilled twice from a sodium–potassium (Na–K) alloy under argon. The Na–K alloy was freshly prepared from a mixture of sodium (Aldrich, 99%) and potassium (Aldrich, 98%). Naphthalene (C<sub>10</sub>H<sub>8</sub>; Fisher, 99.98%), germanium tetrachloride (GeCl<sub>4</sub>; Acros, 99.99%), and *n*-butylmagnesium chloride (MgClBu; Aldrich, 2 M) were used without further purification. HPLC-grade water (EM Science) and HPLC-grade hexane (Aldrich)

were used as received. All chemicals were handled either in a N<sub>2</sub>-filled glovebox or on a Schlenk line using standard anaerobic and anhydrous techniques.

**Sodium Naphthalide [Na(naphth)] Synthesis.** Na metal, 0.5234 g (0.0228 mol), was added to a Schlenk flask in a drybox and transfer to a Schlenk line. Naphthalene (2.920 g, 0.0228 mol) was subsequently added under argon. Approximately 70 mL of freshly distilled and degassed glyme was added to the solids, and the mixture was stirred overnight. The color of the solution changed from colorless to dark green upon the dissolution of Na metal.

**Germanium Nanoparticle Synthesis.** Seventy milliliters of a solution of Na(naphth) was added rapidly via cannula to 0.71 mL (0.00607 mol) of GeCl<sub>4</sub> in 300 mL of glyme in a Schlenk flask at room temperature. The solution immediately changed from a clear solution to a dark brown suspension upon the addition of the Na(naphth) mixture. After being stirred for 10 min, the suspension was allowed to settle. Once settled, a dark brown solid appeared at the bottom of the flask, and a dark yellow solution appeared on the top. The dark yellow solution was transferred via cannula to another Schlenk flask and vacuum-dried, and the naphthalene was sublimed. The dark brown solid was characterized (X-ray diffraction, XRD) to be a combination of amorphous Ge and sodium chloride salt. Freshly distilled and degassed glyme (250 mL) was then added to the flask, followed by 3.1 mL (0.00607 mol) of *n*-BuMgCl. The mixture was left to stir (typically for 12 h) and then pumped down to dryness, extracted with hexane, and rinsed with 1 M HCl and HPLC-grade water. After the removal of hexane and heating under vacuum to remove any residual naphthalene, ca. 500 mg of viscous orange oil (soluble in hexane or chloroform) was obtained. Elemental analysis of the oil is consistent with Ge-(C<sub>4</sub>H<sub>9</sub>)<sub>2.0</sub> (Calculated: Ge, 38.90; C, 51.45; H, 9.65. Experimental: Ge, 30.44; C, 51.54; H, 7.69; Cl, 0.27; Na, <0.01; Mg, <0.01).

**Variations on the Germanium Nanoparticle Synthesis.** Different reaction parameters, such as reductant, time, procedure,

- (19) Vossmeier, T.; Katsikas, L.; Giersig, M.; Popovic, I. G.; Diesner, K.; Chemseddine, A.; Eychmüller, A.; Weller, H. *J. Phys. Chem.* **1994**, *98*, 7665–7673.
- (20) Rossetti, R.; Ellison, J. L.; Gibson, J. M.; Brus, L. E. *J. Chem. Phys.* **1984**, *80*, 4464.
- (21) Rossetti, R.; Hull, R.; Gibson, J. M.; Brus, L. E. *J. Chem. Phys.* **1985**, *82*, 552.
- (22) Henglein, A. *Pure Appl. Chem.* **1984**, *56*, 1215.
- (23) Henglein, A. *Chem. Rev.* **1989**, *89*, 1861–1873.
- (24) Duonghong, D.; Ramsden, J.; Grätzel, M. *J. Am. Chem. Soc.* **1982**, *104*, 2977.
- (25) Hagfeldt, A.; Grätzel, M. *Chem. Rev.* **1995**, *95*, 49–68.



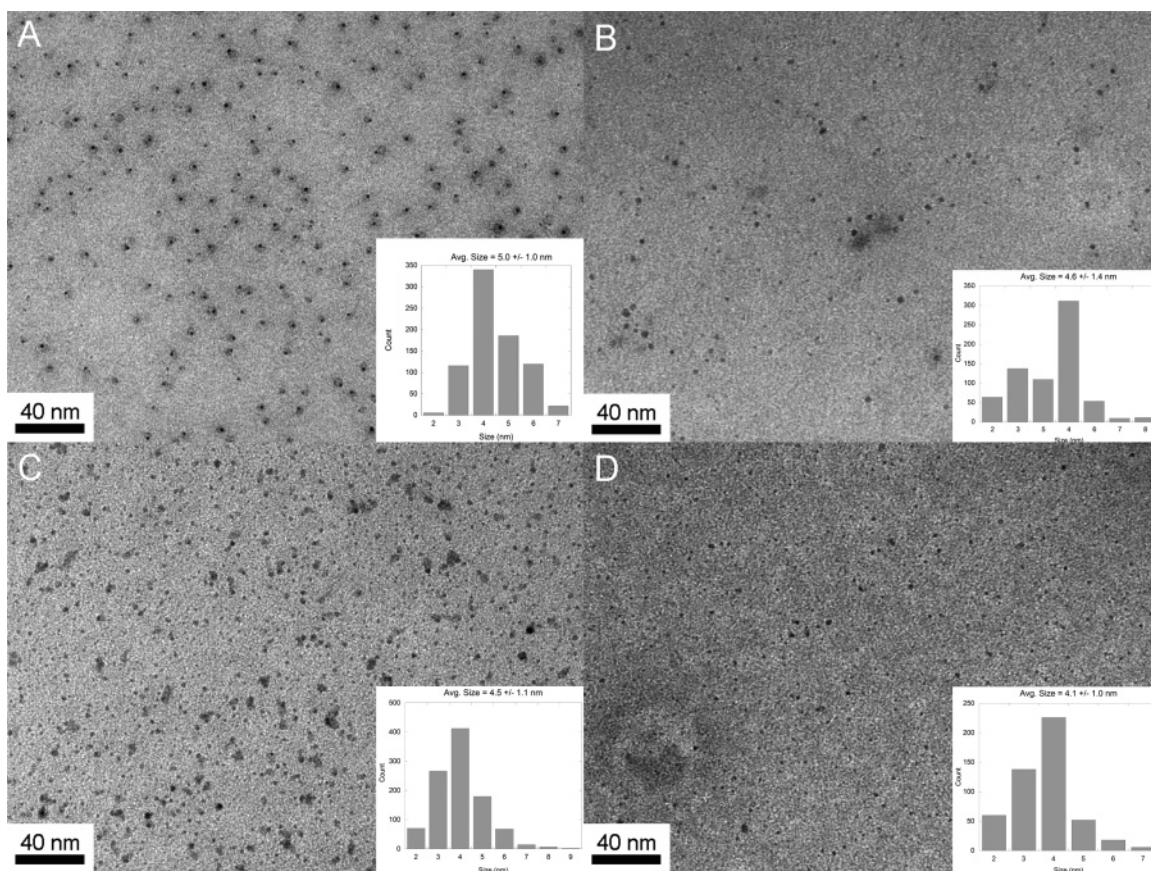


**Figure 2.** Bright-field TEM micrographs of butyl-terminated Ge NPs prepared with stirring times of (A) 10 min, (B) 1 h, (C) 2 h, and (D) 6 h. Insets show size distributions.

concentration, and temperature, were investigated for the production of Ge NPs.

(i) *Reductant.* Lithium, sodium, and potassium metals were used to synthesize alkali metal reductants [Li(naphth), Na(naphth), and K(naphth)]. They were prepared in the manner described above for Na(naphth).

(ii) *Time.* Stirring times of 10 min, 1 h, 2 h, and 6 h were investigated for room-temperature  $\text{GeCl}_4$  and Na(naphth).

(iii) *Procedure.* A one-pot synthesis was explored that did not include removal of any solvent or naphthalene before the final termination step.

(iv) *Concentration.* Dilute (0.07593 M) and concentrated (0.2587 M) mixtures of Na(naphth) in glyme were examined.

(v) *Temperature.* Temperatures for the initial reduction of  $\text{GeCl}_4$  with Na(naphth) were investigated. The Schlenk flask was held at four different temperatures (−40, 0, 30, and 70 °C). Once at the desired temperature, reagents were added, and then the reagent/ $\text{GeCl}_4$ /Na(naphth) mixture was allowed to cool/warm to room temperature. At room temperature, the mixture was left to stir for 1 h, and then the procedure outlined above was followed.

**Characterization.** Transmission electron microscopy (TEM) analyses of the NPs were performed on a Philips CM-12 instrument operating at 100 keV. High-resolution transmission electron microscopy (HRTEM) micrographs were recorded on a Philip CM-200 instrument with a 200-keV accelerating voltage. TEM samples were prepared by dipping holey-carbon-coated, 400-mesh electron microscope grids into the hexane colloid solution and drying them at 120 °C overnight. Chemical analysis was performed at Desert Analytics Laboratory in Tucson, AZ. Powder X-ray diffraction (XRD) data were collected on an INEL CPS120 diffractometer using  $\text{Cu K}\alpha$  radiation.

## Results and Discussion

The production of Ge NPs through the synthesis of  $\text{GeCl}_4$  with sodium naphthalide reduction has been reported.<sup>10,11,13</sup> It was proposed that reaction time was responsible for size differences between NPs of Ge (10- vs 60-min stirring times); however, a large NP size distribution was always observed.<sup>11</sup> This study has discovered that a number of factors contribute to this size distribution. This investigation explores the details of the reaction conditions and characterization of the resulting NP products. All products were examined by TEM.

Starting with a prototypical reaction as described in the Experimental Section [Na(naphth), 12-h stirring time, two-pot synthesis, Na(naphth) in glyme concentration of 0.0775 M, room-temperature reaction, and stoichiometric Na(naphth)/ $\text{GeCl}_4$  ratio of 4:1], the first parameter that was investigated was the effect of the reducing agent. Because the reactivity of alkali metals increases with increasing atomic number, different alkali metal naphthalides were synthesized. The reducing power of the alkali metal naphthalide was found to follow the same trend as their predicted reactivities. The NP synthesis using lithium naphthalide took a minimum of 12 h to complete; therefore, it was too slow and, thus, too mild for our needs. Potassium naphthalide was observed to be the opposite. It was too reactive (reaction was completed too quickly) and immediately formed an amorphous brown precipitate. The reactivity of the original reducing agent, sodium naphthalide, falls between those of Li(naphth) and K(naphth), making it a better reductant for this particular reaction. Hence, for further results presented



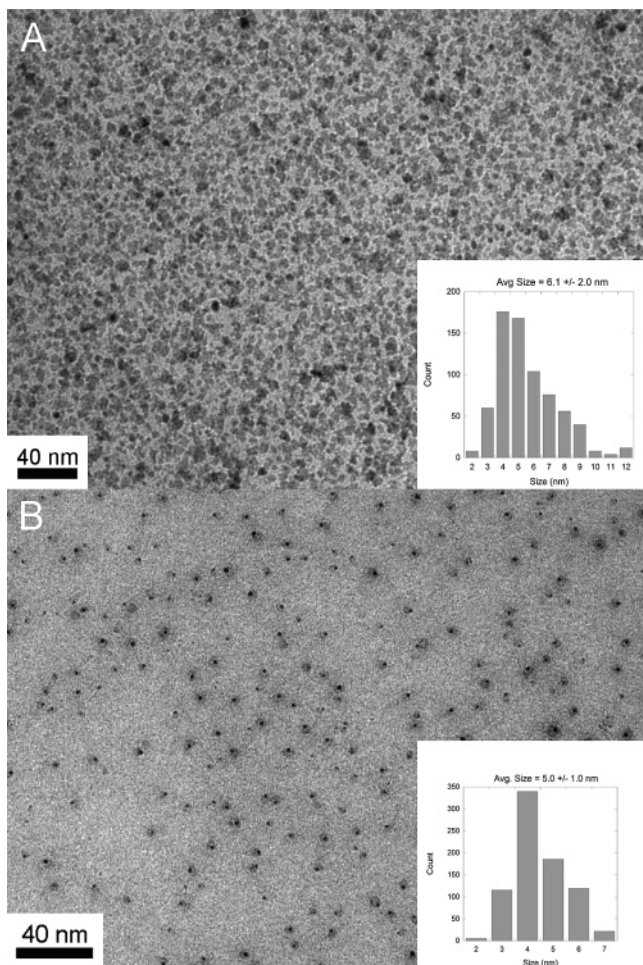


**Figure 3.** Bright-field TEM micrographs of butyl-terminated Ge NPs prepared from (A) one-pot and (B) two-pot synthesis. Insets show size distributions.

in this investigation, Na(naphth) is the reductant that is primarily utilized.

Figure 1A,B presents typical bright- and dark-field micrographs of Ge NPs prepared from a 10-min, one-pot synthesis at 30 °C. The NPs are isolated from each other and well-dispersed on the grid. From the dark-field image, it is clear that the NPs are crystalline because of the visibly bright Bragg orientations.<sup>26</sup> Figure 1C represents the selected-area electron diffraction (SAED) patterns of the NPs, showing four distinct diffraction rings corresponding to the {220}, {311}, {331}, and {440} diffraction planes. These planes are indicative of the diamond cubic lattice of germanium. Figure 1D shows a high-resolution TEM micrograph of a single Ge NP with lattice fringes (2.00 Å) consistent with the {220} planes of diamond-like germanium, indicating highly crystalline NPs. Energy-dispersive X-ray spectroscopy (EDS) analysis confirms the presence of Ge. All samples were analyzed by TEM, and a number were confirmed through elemental analysis. The *n*-butyl-terminated Ge nanoparticles prepared by this route consistently provide a product with the approximate stoichiometry of Ge(C<sub>4</sub>H<sub>9</sub>)<sub>2.0</sub>, which is similar to our previously reported as-prepared Ge NPs.<sup>15</sup> Because the amount of hydrocarbon is much too large

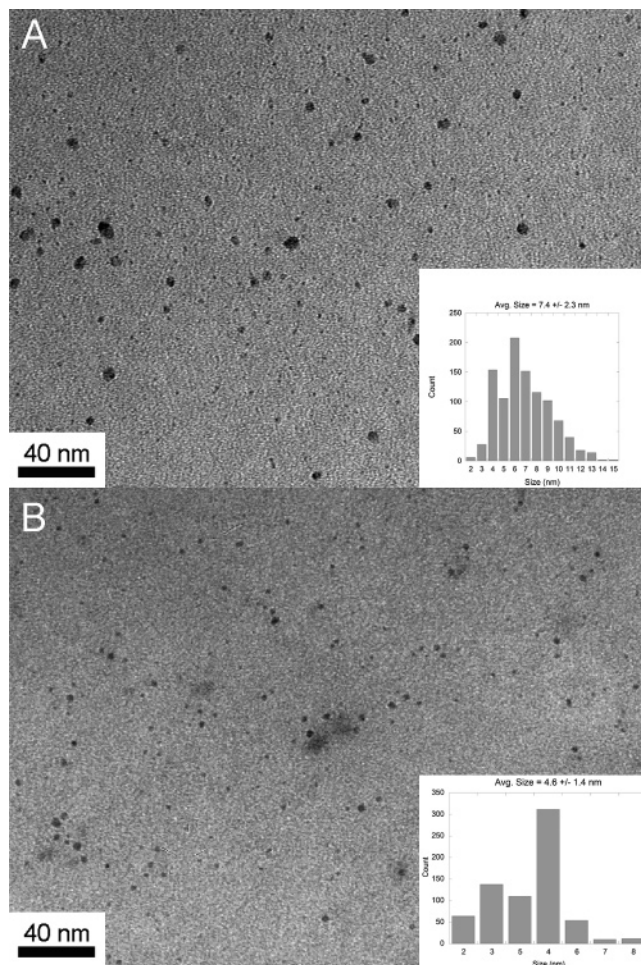


**Figure 4.** Bright-field TEM micrographs of butyl-terminated Ge NPs prepared from (A) concentrated (0.2587 M) and (B) dilute (0.0759) reaction mixtures. Insets show size distributions.

for a monolayer of  $\text{C}_4\text{H}_9$  to form on a 4- or 5-nm-diameter Ge, given the simple surface area and close-packing models, we have suggested that these NPs are dispersed in a hydrocarbon matrix. An X-ray powder diffraction pattern of the oily NP product was not observed. This may be attributed to the NP concentration being too low in the hydrocarbon matrix (based on the elemental analysis provided above). SAED results suggest that the NPs are crystalline; however, it is possible that SAED provides diffraction only of the larger particles.

The second effect that was explored in the investigation of NP growth was reaction time. At room temperature, the NP solution was allowed to stir for various lengths of time before the addition of the Grignard reagent. Data obtained were a collection of various micrographs from reactions with the same stirring times. Figure 2A is a bright-field micrograph of Ge NPs synthesized after 10 min. The histogram inset shows that the average particle diameter is 5.0 nm, with a standard deviation of 1.0 nm based on a random collection of 790 particles. Figure 2B is a bright-field micrograph of Ge NPs synthesized after a 1-h stirring time, displaying an average diameter of 4.6 nm and a standard deviation of 1.4 nm (based on 700 particles). Figure 2C represents the bright-field micrograph of a reaction with a 2-h stirring time, resulting in an average NP diameter of 4.5 nm and a standard

(26) Williams, D. B.; Carter, B. C. *Transmission Electron Microscopy*; Plenum Press: New York, 1996.



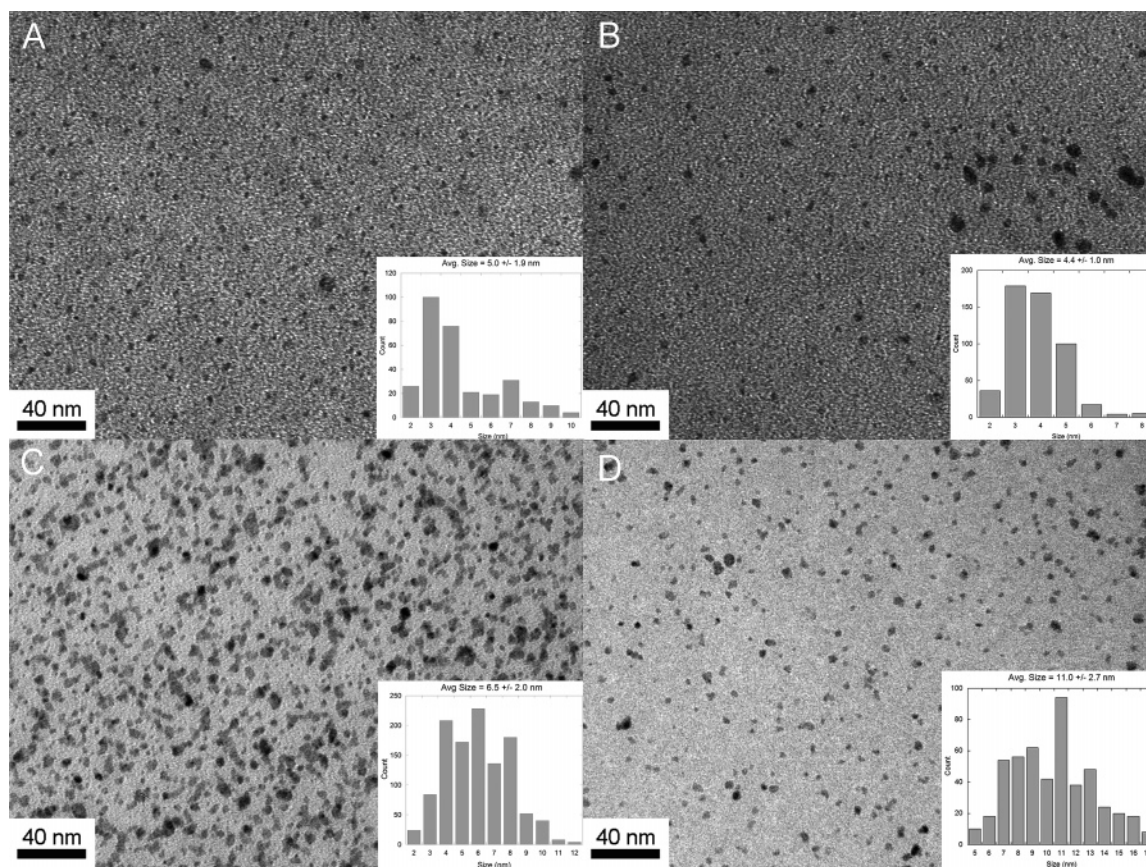


**Figure 5.** Bright-field TEM micrographs of butyl-terminated Ge NPs prepared at (A)  $-40$ , (B)  $0$ , (C)  $30$ , and (D)  $70$   $^{\circ}\text{C}$ . Insets show size distributions.

deviation of  $1.1$  nm (based on 1017 particles). Figure 2D is the bright-field micrograph of a 6-h Ge NP stirring time. The resulting average NP diameter for this time variation was found to be  $4.1$  nm, with a standard deviation of  $1.0$  nm (based on 500 particles). EDS analysis for each of these stirring times confirms the presence of Ge. The smallest percent standard deviation is obtained when the reaction mixture is stirred for the shortest length of time. According to La Mer and Dinegar's nucleation theory<sup>16</sup> and our results, this reaction reaches its saturation within 10 min of stirring. The Ge NP average diameter sizes for all stirring times are within 80% of each other, which suggests a uniform NP growth after nucleation takes place.

The motivation for studying the third effect in this investigation stems from the interest in simplifying the overall synthesis of Ge NPs. For most of the reactions presented, a "two-pot" synthetic procedure was used where the solvent and naphthalene were removed prior to the addition of the Grignard reagent. In some cases, however, we investigated the effects on the synthesis of not removing the naphthalene until the final steps (after the addition of the Grignard), referred to as a "one-pot" procedure. A one-pot synthesis is preferred when a larger scale is needed. Figure 3A shows a bright-field micrograph image of the results of a one-pot reaction. The histogram of NP size distribution is included as an inset. The average NP diameter is  $6.1 \pm 2.0$  nm based on 712 particles. Figure 3B is a bright-field micrograph of the results of a two-pot synthesis (the size distribution is shown in the inset), giving an average NP diameter of  $5.0 \pm 1.0$  nm (based on 790 particles). EDS

analyses of all samples confirm the presence of Ge. The two-pot synthesis results in a smaller average NP size and narrower size distribution than the one-pot synthesis (20% standard deviation vs 33%). This might be due to the loss of a contributing side reaction during the removal of all volatile byproducts under vacuum before surface termination.

According to La Mer and Dinegar's nucleation theory,<sup>16</sup> the precursor concentration is an important factor that controls the size production of NPs. Therefore, as the fourth variation parameter, we explored the effects of concentration for a 1-h stirring time in a two-pot synthesis. Figure 4A shows a bright-field micrograph of Ge NPs prepared from concentrated  $\text{GeCl}_4$  ( $0.2587$  M). The resulting average particle size was found to be  $7.4 \pm 2.3$  nm (based on 1016 particles). Figure 4B is a bright-field micrograph of Ge NPs prepared from a dilute  $\text{GeCl}_4$  solution ( $0.0759$  M), which produced an average particle diameter of  $4.6 \pm 1.4$  nm (based on 700 particles). EDS analysis confirms the presence of Ge. The less concentrated reaction results in a smaller average NP. As evidenced, the size percentage standard deviations are similar for the two concentrations, suggesting that nucleation and growth are occurring almost simultaneously. The concentrated reaction mixture has a polydispersity of  $\sim 31\%$ , and the dilute solution reveals a similar polydispersity of  $\sim 30\%$ . According to La Mer and Dinegar,<sup>16</sup> it is expected that a higher percentage of nonuniform growth and polydispersion will be observed when the initial solutions are concentrated.<sup>2</sup> For the concentrated sample in this study, the rate of Ge seed production becomes high, thus producing a larger average NP size. The size distributions for the two

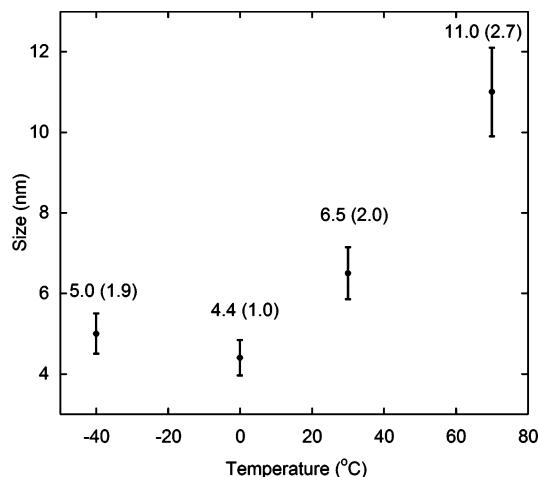


**Figure 6.** Plot of NP size as a function of reaction temperature. The standard deviation is included in the error bars.

cases are very similar, and 80% of the NPs are close to the average size.

In continuing our exploration of the effects on size control, the fifth altered parameter was reaction temperature. For this study, the stirring time (10 min) and concentration (0.093 M) were kept constant, and a one-pot synthesis was employed. For low-temperature evaluation, the solution mixtures were cooled to  $-40$  and  $0$  °C using a dry-ice-acetone bath. For room- to moderate-temperature analysis, the solution mixtures were heated using a temperature-controlled heating mantle. Figure 5A is a bright-field micrograph of Ge NPs prepared at  $-40$  °C. The average NP size was found to be  $5.0 \pm 1.9$  nm (based on 300 particles). Figure 5B shows the bright-field image of particles prepared at  $0$  °C, indicating an average diameter of  $4.4 \pm 1.0$  nm (based on 510 particles). Figure 5C illustrates a bright-field image of particles synthesized at  $30$  °C, resulting in an average diameter of  $6.5 \pm 2.0$  nm (based on 1136 particles). Figure 5D represents the bright-field image of particles synthesized at  $70$  °C. This temperature results in an average NP diameter of  $11.0 \pm 2.7$  nm (based on 492 particles). EDS analysis confirms the presence of Ge.

Figure 6 is a plot of particle size as a function of temperature. From this plot, it is clear that smaller size distributions are obtained at lower temperatures. The chemical potential can be increased by decreasing the solubility of germanium tetrachloride in the solution, which is achieved by lowering the overall temperature of the system. This will result in one brief outburst of nuclei, leaving enough dissolved germanium to produce diffusional growth.<sup>16</sup> We can see from this plot that, at lower temperatures ( $-40$  and  $0$  °C), the average sizes are much smaller than at higher temperatures ( $30$  and  $70$  °C). The standard deviations of the size distributions for these NPs are comparable to each other, and  $\sim 80\%$  of the NPs are within the average size.

## Summary

On the basis of TEM micrographs of various samples synthesized under various reaction conditions, we can conclude that NP nucleation is most influenced by variations of reductant, concentration, temperature, and synthesis. For temperatures other than room temperature, it was observed that the Ge NPs quickly achieve their maximum size based on their concentration. Reaction stirring time (1 h vs 10 min at room temperature) does not appear to dramatically alter the average NP size. The reaction is complete in the first 10 min, suggesting that even shorter stirring times are worthy of further investigation.

Growth of Ge NPs follows similar kinetics at room temperature as does the groups II–VI NP synthesis at high temperatures: a short and fast nucleation and subsequent growth. These results also suggest that control over NP growth can be achieved by changing temperature and solvent.

**Acknowledgment.** We thank Dr. Richard Baldwin for his initial work on this project and Professor Frank Osterloh and Shawna Brown for useful discussions. This research was funded in part by NIST ATP, NSF DMR-0120990, CHE-0304871, and AFOSR 03NE141.

CM0521222